Kurzmack, M., Verjovski-Almeida, S., & Inesi, G. (1977) *Biochem. Biophys. Res. Commun. 78*, 772–776.
Lowry, O. H., Rosebrough, N. J., Farr, A. L., & Randall, R. J. (1951) *J. Biol. Chem. 193*, 263–275.
MacLennan, D. H., & Holland, P. C. (1975) *Annu. Rev. Biophys. Bioeng. 4*, 377–404.
McCray, J. A., Herbette, L., Kihara, T., & Trentham, D. R. (1980) *Proc. Natl. Acad. Sci. U.S.A. 77*, 7237–7241.
McFarland, B. H., & Inesi, G. (1971) *Arch. Biochem. Biophys. 145*, 456–464.
Pierce, D. H. (1982) Ph.D. Dissertation, University of Pennsylvania, Philadelphia, PA.
Scarpa, A. (1979) *Methods Enzymol. 56*, 301–338.
Scarpa, A., & Inesi, G. (1972) *FEBS Lett. 22*, 273–276.
Scarpa, A., Baldassare, J., & Inesi, G. (1973) *J. Gen. Physiol. 60*, 735–749.
Simon, W., Morf, W. E., & Ammon, D. (1977) in *Calcium Binding Proteins and Calcium Function* (Wasserman, R. H., Corradino, R. A., Carafoli, E. Kretsinger, R. H., MacLennan, D. H., & Siegel, F. L., Eds.) pp 50–62, Elsevier, New York.
Strehler, B. L. (1968) *Methods Biochem. Anal. 16*, 99–181.
Sumida, M., & Tonomura, Y. (1974) *J. Biochem. (Tokyo) 75*, 283–297.
Takakuwa, Y., & Kanazawa, T. (1981) *J. Biol. Chem. 256*, 2691–2700.
Verjovski-Almeida, S., Kurzmack, M., & Inesi, G. (1978) *Biochemistry 17*, 5006–5013.
Yamada, S., Yamamoto, T., & Tonomura, Y. (1970) *J. Biochem. (Tokyo) 67*, 789–794.
Yamamoto, T., Takisawa, H., & Tonomura, Y. (1979) *Curr. Top. Bioenerg. 9*, 179–236.

Distance Measurement between the Active Site and Cysteine-177 of the Alkali One Light Chain of Subfragment 1 from Rabbit Skeletal Muscle†

Diana J. Moss‡ and David R. Trentham*

ABSTRACT: Förster energy-transfer techniques have been applied to labeled myosin subfragment 1 from rabbit skeletal muscle to determine an intramolecular distance and whether this distance changes during magnesium-dependent ATPase activity. The alkali one light chain was labeled at Cys-177 with *N*-(iodoacetyl)-*N'*-(5-sulfo-1-naphthyl)ethylenediamine (1,5-IAEDANS) and then exchanged into subfragment 1. High specificity of labeling was indicated by high-performance liquid chromatography analysis of a tryptic digest of the labeled light chain. 2'(3')-*O*-(2,4,6-Trinitrophenyl)adenosine 5'-diphosphate (TNP-ADP) was bound to the labeled protein at the ATPase active site. The efficiency of energy transfer between the probes was 0.09 when measured by both steady-state and time-resolved fluorescence. Anisotropy measurements of the bound AEDANS indicated considerable freedom of motion of the probe. The probable distance between the probes was 57 Å. This distance was unchanged during triphosphatase activity. Two further sites of TNP-ADP interaction with subfragment 1 were found. The effect of these interactions on the energy-transfer measurements was reduced to a minimum by careful choice of reaction conditions.

The myosin and actomyosin ATPase[1] mechanisms have been intensively studied to characterize the intermediates and measure their rates of interconversion (Trentham et al., 1976; Taylor, 1979). This has led to a detailed description of the hydrolysis of ATP (Webb & Trentham, 1983).

$$\mathrm{M} + \mathrm{ATP} \overset{1}{\rightleftharpoons} \mathrm{M{\cdot}ATP} \overset{2}{\rightleftharpoons} \mathrm{M^*{\cdot}ATP} + \mathrm{H_2O} \overset{3}{\rightleftharpoons} \mathrm{M^{**}{\cdot}ADP{\cdot}P_i} \overset{4}{\rightleftharpoons} \mathrm{M^*{\cdot}ADP{\cdot}P_i} \overset{5}{\rightleftharpoons} \mathrm{M^*{\cdot}ADP} + \mathrm{P_i} \overset{6}{\rightleftharpoons} \mathrm{M{\cdot}ADP} \overset{7}{\rightleftharpoons} \mathrm{M} + \mathrm{ADP} \quad (1)$$

Equation 1 shows a seven-step mechanism for the myosin ATPase in which the asterisks are used to distinguish intermediates. In eq 1 conformation changes (steps 2, 4, and 6), which have so far been characterized predominantly by kinetic methods, are associated with substrate binding and the release of each product. The nature of the conformation changes implied in the myosin and actomyosin ATPase mechanisms is not understood. It is not clear, for example, whether the conformation changes have a direct role in contraction, possibly through the movement of large segments of protein, or whether their role is more indirect and is limited to small perturbations of structure in the vicinity of the ATPase active site.

Many techniques have been used to probe the structural features of actin and myosin. Of these, utilization of Förster energy transfer is especially promising as a means to determine the relative location of points of interest and to examine the size and extent of the inter- and intramolecular protein motion (Stryer, 1978). Over the past few years several measurements

† From the Department of Biochemistry and Biophysics, University of Pennsylvania School of Medicine, Philadelphia, Pennsylvania 19104. *Received March 15, 1983.* Supported by grants from the National Institutes of Health (AM 23030), the Muscular Dystrophy Association of America, and Whitehall Foundation. This work has been described in part in Moss & Trentham (1980).

‡ Present address: MRC Cell Biophysics Unit, London WC2B 5RL, U.K.

[1] Abbreviations: ATPase, adenosine-5'-triphosphatase; TNP-ADP, 2'(3')-*O*-(2,4,6-trinitrophenyl)adenosine 5'-diphosphate (other TNP containing compounds are similarly abbreviated); 1,5-IAEDANS, *N*-(iodoacetyl)-*N'*-(5-sulfo-1-naphthyl)ethylenediamine; A1 and A2 light chains, the alkali one and alkali two light chains of myosin (Weeds & Pope, 1977); S1A1 and S1A2, subfragment 1 containing A1 and A2 light chains, respectively; A1-AEDANS light chain, A1 light chain labeled at Cys-177 with 1,5-IAEDANS (other 1,5-IAEDANS-labeled species are similarly abbreviated); DEAE, diethylaminoethyl; DTNB, 5,5'-dithiobis(2-nitrobenzoic acid); EDTA, ethylenediaminetetraacetic acid; Tris, tris(hydroxymethyl)aminomethane; HPLC, high-performance liquid chromatography.

0006-2960/83/0422-5261$01.50/0

which rely on Förster energy transfer have been made within actomyosin or its components (Morales et al., 1982).

Measuring protein structure changes is more difficult, and so most studies have concentrated on subfragment 1, the smallest protein component of the actomyosin system containing the ATPase active site in viable form. Several chemical and spectroscopic studies of subfragment 1 have identified differences in structure between subfragment 1, M**·ADP·P_i, and M*·ADP, especially in the vicinity of the ATPase active site [reviewed by Morales et al. (1982)]. Altered reactivity of the reactive thiol "SH_1" in the presence of nucleotide (Watterson et al., 1975), chemical cross-linking between thiols "SH_1" and "SH_2" (Burke & Reisler, 1977), and the ability to trap ADP at the active site by cross-linking (Wells & Yount, 1979) provide evidence for conformational changes and also give the scale of the conformation changes occurring around the active site due to nucleotide binding. How far these changes are transmitted through the protein is not known, although circular dichroism measurements suggest there is little change in the helix and pleated-sheet content (Gratzer & Lowey, 1969).

This paper reports the measurement of the distance between the active site and Cys-177, the single thiol of the alkali one light chain (Frank & Weeds, 1974), by using Förster energy transfer and whether there is a change in this distance in going from one intermediate of the ATPase mechanism to another.

Förster energy-transfer techniques require the specific incorporation of two chromophoric probes into subfragment 1 at least one of which must be fluorescent. In order to achieve as high a degree of specificity as possible, it was decided to introduce the probes at the ATPase active site and at the thiol group of the alkali light chains of subfragment 1. The two probes used were an analogue of ADP, TNP-ADP, which binds at the active site, and 1,5-IAEDANS, which could be specifically reacted with the single thiol of isolated alkali light chains and then incorporated into subfragment 1 (Wagner & Weeds, 1977). The interactions of TNP-ADP and TNP-ATP with subfragment 1 were examined to determine specificity and to compare properties of the protein in the presence of the two nucleotides. TNP-ADP was shown to bind tightly at the active site and weakly at a second site and to react at a third site. Conditions were found where TNP-ADP was bound mainly at the active site and its presence at the other two sites was insignificant. The specificity of the reaction of 1,5-IAEDANS with the alkali one light chain was also investigated.

A second problem in using Förster energy transfer is the assumption of a value for K^2, the orientation factor between donor and acceptor dipoles. This is usually taken to be $^2/_3$, the value for two freely rotating probes. To determine the reasonableness of this approximation, the rotational mobility of the AEDANS group relative to subfragment 1 was examined by time-dependent anisotropy measurements.

Materials and Methods

Preparation of Proteins. Rabbit skeletal myosin light chains were dissociated from the heavy chains essentially by the method of Weeds (1976). The alkali light chains were separated from the DTNB light chains by precipitation using 25% ethanol (Perrie et al., 1973). The concentration of light chains was determined by the biuret method.

Subfragment 1 was prepared as S1A1 and S1A2 by using chymotryptic digestion of myosin as described by Weeds & Taylor (1975) except that the ionic strength of the myosin solution was reduced by 4-fold dilution rather than by dialysis, and the myosin rods and undigested myosin were precipitated by 2.5-fold dilution. This enabled S1A1 and S1A2 to be prepared and separated in 2 days. The concentration of subfragment 1 was determined by using $\epsilon^{1\%}_{280nm} = 7.6$ cm^{-1} (Weeds & Pope, 1977). The K^+-ATPase of the proteins was routinely measured and was 10–16 s^{-1} at 20 °C and pH 8.0.

Labeling of Alkali Light Chains. Solid 1,5-IAEDANS at a final concentration of 10 mM was added to a mixture of A1 and A2 light chains (5 mg/mL) in 0.1 mM dithiothreitol, 0.1 mM EDTA, 0.1 mM NaN_3, 5 M guanidine hydrochloride, and 50 mM Tris-HCl at pH 8 and 23 °C. The pH was maintained at 8 by the addition of 1 M Tris base (Marsh & Lowey, 1980). The reaction was allowed to proceed at 23 °C in the dark for 1.5 h at which point the reaction was terminated by the addition of 2-mercaptoethanol to a final concentration of 100 mM. The mixture was dialyzed against 0.1 mM EDTA, 0.1 mM NaN_3, and 50 mM Tris-HCl at pH 8 and 4 °C. The A1 and A2 light chains were separated, and the remaining free label was removed by ion-exchange chromatography on a DEAE-cellulose column (Cl^- form) (2.4-cm diameter × 45 cm) using a 2-L linear gradient of 0.1–0.3 M NaCl in 0.1 M urea and 50 mM Tris-HCl at pH 8 and 4 °C. The stoichiometry of labeling was determined spectrophotometrically from the relative concentration of incorporated AEDANS ($\epsilon_{335nm} = 6.3 \times 10^3$ M^{-1} cm^{-1}) and protein (determined by the biuret method). The stoichiometry of incorporation was in the range 0.6–1.1 molecules of AEDANS incorporated per subfragment A1 light chain.

Exchange of Light Chains. The labeled light chains were exchanged by the method of Wagner & Weeds (1977). In a typical exchange 50 μM S1A1 and 250 μM A1-AEDANS were mixed in 1 mM dithiothreitol, 1 mM EDTA, and 0.1 M imidazole hydrochloride at pH 7 and 0 °C. Solid NH_4Cl was added slowly to a final concentration of 4.7 M (assuming a volume change of 20%). The solution was stirred at 0 °C for 20 min at which point the NH_4Cl was removed by dialysis for 5 h against 0.1 mM dithiothreitol, 0.1 mM EDTA, 0.1 mM NaN_3, and 50 mM Tris-HCl at pH 8 and 4 °C. The solution was applied to a DEAE-cellulose column (Cl^- form) (1.4-cm diameter × 30 cm) equilibrated in 50 mM Tris-HCl at pH 7.6. The protein was eluted with a 500-mL linear gradient of 0–120 mM KCl in 50 mM Tris-HCl at pH 7.6 and 4 °C at a flow rate of 0.5 mL/min. The fluorescence intensity of the fractions was measured by using a Farrand Mark 1 fluorometer with exciting light at 345 nm and emission detection at 495 nm. S1A1-AEDANS was used within 48 h of preparation during which time the K^+-ATPase activity remained fairly constant, decreasing by <20%. S1A1-AEDANS could be stored in vials in liquid nitrogen without loss of ATPase activity.

Preparation and Analysis of Tryptic Peptides from A1-AEDANS Light Chains. A1-AEDANS light chains (2–4 mg/mL) were dialyzed extensively against water. The A1-AEDANS light chains were digested by trypsin with the aid of a pH stat to monitor the extent of reaction and to control the pH. The pH of the solution was adjusted to pH 8.7, and trypsin solution (1 mg/mL dissolved in 1 mM HCl) (Smyth, 1967) was added to give 1:50 by weight trypsin to light chain. The pH maintained by controlled addition of 50 mM KOH. Samples were removed, rapidly frozen, lyophilized, and dissolved in 0.1% H_3PO_4 for HPLC analysis.

Tryptic peptides were analyzed by HPLC with a reverse-phase C_{18} analytical column (Waters). The column was equilibrated in 0.1% H_3PO_4. Following sample injection the column was washed with 0.1% H_3PO_4 for 10 min. Then peptides from 300 μg of protein were eluted with a linear gradient of 0.1% H_3PO_4 to 0.1% H_3PO_4–CH_3CN (40:60 v/v)

over 1 h at a flow rate of 2 mL/min. The eluant was monitored at 335 nm.

Polyacrylamide Gel Electrophoresis. Proteins were examined on slab gels by using 10% polyacrylamide gel electrophoresis in the presence of 0.1% sodium dodecyl sulfate (Weeds & Pope, 1977) but with a Tris–glycine buffer at pH 8.8. Fluorescent bands were observed by illumination with a long wavelength ultraviolet lamp and were photographed by using a Polaroid MP3 camera and a Series 6 Wratten K2 filter. To detect protein, the gels were stained in 0.5% Coomassie brilliant blue in methanol–acetic acid–water (45:10:45 v/v) and destained in the same solvent.

TNP Analogues. TNP-adenosine was prepared by mixing 0.02 M adenosine with 0.1 M trinitrobenzenesulfonic acid in water at pH 9.5 (Azegami & Iwai, 1964). The pH of the reaction mixture was maintained by addition of 0.5 M NaOH, and the reaction was left overnight at room temperature. The solution was acidified to pH 4 with 1 M HCl at which point the neutral form of the product precipitated out and was collected by filtration.

TNP-ADP and TNP-ATP were synthesized from ADP and ATP by a similar method and purified on DEAE-cellulose (HCO_3^- form) (Hiratsuka & Uchida, 1973). The compounds were characterized from their spectra due to the Meisenheimer complex ($\epsilon_{408nm} = 2.61 \times 10^4\ M^{-1}\ cm^{-1}$). TNP-ADP was also obtained from Molecular Probes Inc., Plano, TX.

The purity of the nucleotides was checked by HPLC with a weak anion-exchange column [Waters (NH_2)-Bondapak] and 0.1 M $(NH_4)H_2PO_4$ as eluting solvent at pH 4.0.

Spectroscopic Measurements. Absorption spectra were measured with a Cary 118 spectrophotometer. Fluorescence measurements were carried out on a SLM 8000 single photon counting fluorometer equipped with a cooled Hamamatusu R928 red-sensitive photomultiplier. Continuous fluorescence titration curves were obtained with the aid of a Sage syringe pump 341A which dispensed 0.2 μL/min from a 10-μL Hamilton syringe. The cuvette contents were continuously mixed by a magnetic stirrer at 15 °C. Transient kinetic measurements were made on a stopped-flow fluorometer as described by Whitaker et al. (1974). The experiments were performed at 15 °C with a temperature-controlled stopped-flow block.

Fluorescent lifetimes were measured by using an Ortec photon counting nanosecond fluorometer as described by Vanderkooi et al. (1977). An ultraviolet filter transmitting light from 320 to 390 nm was used in the excitation light beam and a GG420 Schott filter which cut off light below 420 nm was used on the emission side. The lifetime measurements were made on 0.1 mL of solution in a 2 mm × 2 mm pathlength cuvette at 15 °C. The data took 10–15 min to collect in each case. This time is sufficiently short so that, when 1 mM ATP was included in a solution containing subfragment 1, some ATP remained at the end of the experiment. The sample decay curves were deconvoluted from the lamp flash by using a Laplace transform method (Gafni et al., 1975). Time-dependent anisotropy measurements were also obtained by using the Ortec nanosecond fluorometer with modifications as described by Dixit et al. (1982).

Determination of the Quantum Yield. The quantum yield of AEDANS covalently attached to subfragment 1 was determined by a method based on that of Parker (1968). The absorption, Δ_1, of a solution of quinine bisulfate (approximately 1 μM) in 0.05 M H_2SO_4 was measured at 340 nm in a Beckman DU 8 spectrophotometer. The complete uncorrected emission spectrum was obtained by exciting at 340 nm. This

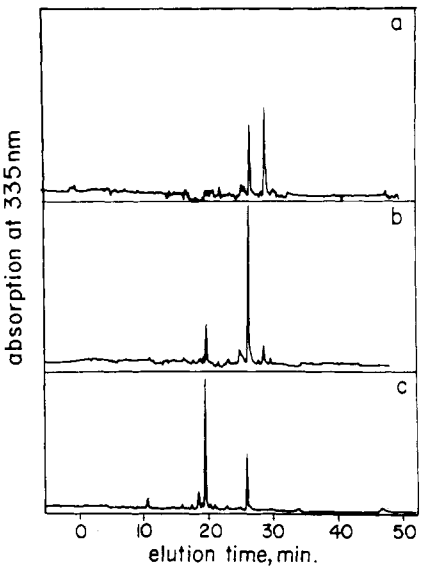

FIGURE 1: HPLC analysis of tryptic peptides of A1-AEDANS light chain. A1-AEDANS light chain (104% labeled protein) was digested with trypsin as described under Materials and Methods. (a) 70% digested, (b) 85% digested, and (c) b digested for a further 3 h. Zero time indicates the start of the elution gradient.

was repeated for a solution of S1A1-AEDANS of similar absorption, Δ_2. All measurements were at 15 °C. The quantum yield, ϕ_1, of the quinine bisulfate was taken as 0.7 (Scott et al., 1970), and so by use of the following equation, in which the areas relate to corrected spectra, the quantum yield of the AEDANS, ϕ_2, could be estimated as follows:

$$\frac{\text{area under emission curve 1}}{\text{area under emission curve 2}} = \frac{\Delta_1\phi_1}{\Delta_2\phi_2}$$

Hudson & Weber (1973) measured the lifetime and quantum yield of 1,5-IAEDANS in a number of water–ethanol mixtures. For mixtures up to 60% ethanol there was a linear relationship between quantum yield and the lifetime. The lifetime of S1A1-AEDANS was measured to be 14.0 ns, and this was also used to estimate the quantum yield.

N-Ethylmaleimide Labeling of Subfragment 1. Subfragment 1, 134 μM, was mixed with 450 μM [^{14}C]-*N*-ethylmaleimide (1 mCi/mmol) for 20 min in 50 mM Tris-HCl at pH 8 and 0 °C. The reaction was quenched with 10 mM dithiothreitol. The stoichiometry of labeling was 1:1.7. The K^+-ATPase activity had fallen to 11.5%, and the Ca^{2+}-ATPase activity had risen to 224% of control values which is consistent with predominant labeling of the SH_1 thiol.

Results

Incorporation of Donor (AEDANS) into Subfragment 1. Preliminary studies established that it was preferable to work with A1-AEDANS light chains for two reasons. First, it was possible to obtain the A1 light chain in larger amounts than the A2 light chain, and second, A2-AEDANS light chain cochromatographed with a significantly quantity of a low molecular weight derivative of AEDANS.

The specificity of labeling was investigated by trypsin hydrolysis of the light chains and examination of the peptides by HPLC. Preliminary experiments showed that more than one 335 nm absorbing (i.e., AEDANS containing) peptide was obtained. The time course of trypsin digestion was therefore examined. Figure 1 shows the elution profiles of samples which had been subjected to varying degree of tryptic digestion. The labeling appears to be specific but with the peptide containing AEDANS being progressively digested during proteolysis.

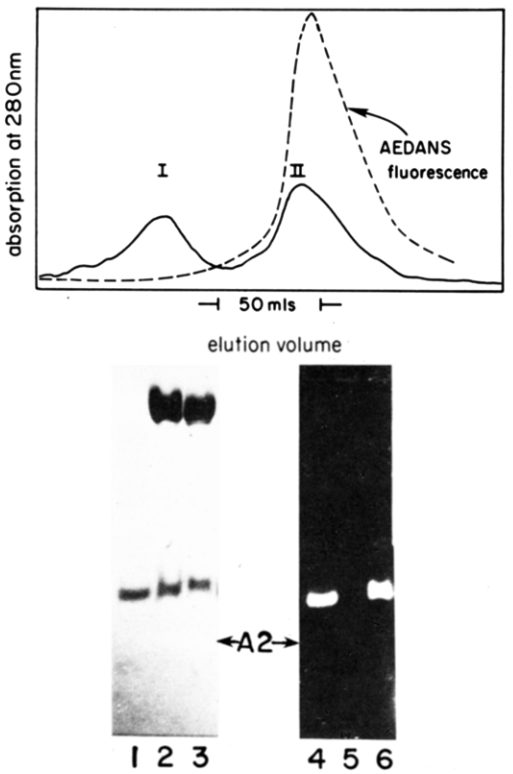

FIGURE 2: (Top) Elution profile of S1A1-AEDANS. Peak I was characterized as unlabeled S1A1 and peak II as S1A1-AEDANS. (Bottom) 10% polyacrylamide gel electrophoresis in the presence of 0.1% sodium dodecyl sulfate of A1-AEDANS light chain (gels 1 and 4), pooled fractions of peak I (gels 2 and 5), and pooled fractions of peak II (gels 3 and 6). Gels 1–3 were stained with Coomassie brilliant blue. Gels 4–6 show AEDANS fluorescence on long wavelength ultraviolet irradiation. The mobility of the A2 light chain is indicated.

Thus, a peak containing AEDANS appeared with a 29-min elution time after starting the gradient (Figure 1a) to be followed on further digestion by a peak at 26 min (Figure 1a–c) and then by a peak eluted after 19 min (Figure 1b,c).

Initially S1A2 was used for the exchange with the A1-AEDANS light chain, since it was thought that S1A1-AEDANS and S1A2 could be separated in the same way as unlabeled subfragment 1. However, the fluorescent label changed the mobility of S1A1 such that it eluted with or a little after S1A2. The best separation was obtained between S1A1 and S1A1-AEDANS, and so S1A1 was used as the starting material for all further experiments. The clean separation of S1A1 and S1A1-AEDANS and the relatively constant fluorescence to 280-nm absorption ratio across the S1A1-AEDANS elution peak suggest that labeling was greater than 90% of the alkali light chain thiol (Figure 2, top). Polyacrylamide gel electrophoresis of eluted samples showed that fluorescence was specifically associated with a single light chain component (Figure 2, bottom). Coomassie blue staining (Figure 2, bottom) showed that the S1A1-AEDANS contained a single light chain with identical electrophoretic mobility with that characterized by fluorescence. The K^+-ATPase activity of labeled subfragment 1 was not affected by incorporation of the label in agreement the results of Marsh & Lowey (1980).

Interaction of TNP-nucleotides and TNP-adenosine with Subfragment 1. The stoichiometry and specificity of TNP-ADP binding to subfragment 1 were analyzed as a necessary preliminary to the energy-transfer measurements. A binding site with $K_D = 0.3$ μM was identified from titration experiments in which the intrinsic protein fluorescence was quenched through TNP-ADP binding (Figure 3).

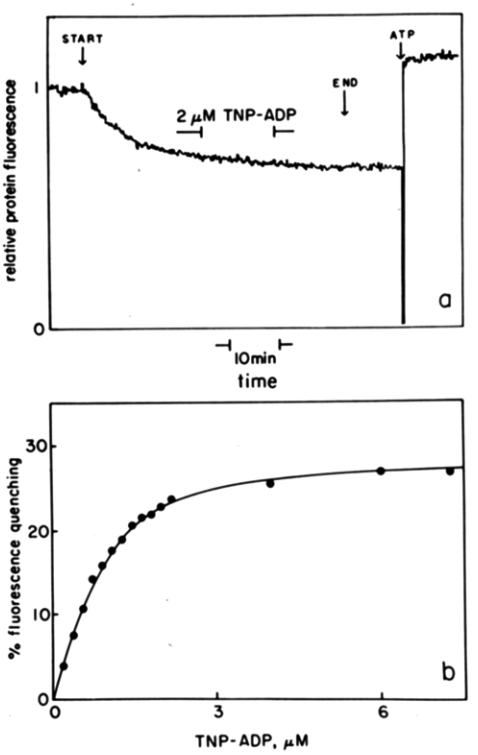

FIGURE 3: (a) Titration of TNP-ADP into S1A1 by using protein fluorescence. TNP-ADP was titrated at a rate of 0.14 μM/min into 2 mL of 1 μM S1A1 in 0.1 M KCl, 5 mM $MgCl_2$, and 50 mM Tris-HCl at pH 8 and 15 °C. Wavelengths of excitation and emission were 300 and 340 nm, respectively, thus reducing as much as possible the inner filter effects due to the TNP-ADP absorption. The final optical densities were 0.037 (300 nm) and 0.018 (340 nm). The quenching due to absorption was estimated to be 10% by displacement of TNP-ADP from the active site of S1A1 by ATP (see figure) and also by addition of 7.25 μM TNP-adenosine. (b) The dissociation constant, K_D, of TNP-ADP binding to S1A1. The data points were calculated from the titration curve by subtracting a background slope corresponding to 10% quenching. The line is the theoretical curve for $K_D = 0.3$ μM with a maximum fluorescence change of 29%.

The K_D was obtained by simulating curves by using the equation

$$K_D/(1 - \alpha) = [L_0]/\alpha - [E_0]$$

where $[L_0]$ = total ligand concentration, $[E_0]$ = total subfragment 1 concentration, and α = the fraction of subfragment 1 sites containing bound ligand.

When TNP-ADP was present in solution with subfragment 1 under conditions where almost all the TNP-ADP was bound at the ATPase active site, very little change was observed in the TNP fluorescence. This is surprising in view of the TNP fluorescence enhancement reported by Hiratsuka (1976). This point was therefore investigated further.

In more concentrated solutions of TNP-ADP and subfragment 1 a large enhancement of TNP fluorescence was observed. This fluorescence was also seen in the presence of ATP or when TNP-adenosine rather than TNP-ADP was added, suggesting there is a second binding site for TNP-ADP that is weaker in affinity than at the active site and is probably due to binding of the TNP moiety. The properties of this second binding site were investigated by using TNP-adenosine since TNP-adenosine was less likely to bind at the active site than TNP-ADP, and the TNP fluorescence was more marked with TNP-adenosine than with TNP-ADP.

TNP-adenosine was titrated into 20 μM subfragment 1. At the high concentrations necessary to observe the TNP fluorescence inner filter effects were large and contributed to the nonlinear increase in TNP fluorescence (Figure 4). From

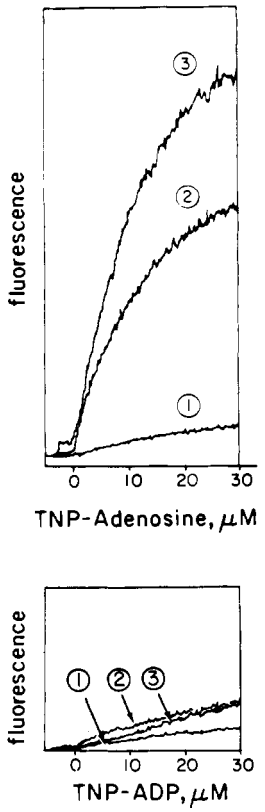

FIGURE 4: Titration of TNP-adenosine and TNP-ADP with S1A1 by using TNP fluorescence. TNP-adenosine (upper traces) and TNP-ADP (lower traces) were titrated into 1.5 mL of (1) 0.1 M KCl, 5 mM $MgCl_2$, and 50 mM Tris-HCl at pH 7.6 and 15 °C (buffer A), (2) 20 μM S1A1 in buffer A, and (3) 20 μM S1A1 and 3 mM ATP in buffer A. The fluorescence scale is the same in both cases. Wavelengths of excitation and emission were 500 and 540 nm, respectively, and the final absorbance was 0.45 (500 nm) and 0.025 (540 nm).

these data, a lower limit of 30 μM may be estimated for the dissociation constant of TNP-adenosine to the protein.

An interesting point is the difference between the titration in the presence and absence of ATP (Figure 4). It is not clear whether this was due to a change in TNP affinity to the protein or a change in fluorescence of the protein-bound TNP. Direct competition for the TNP site by ATP was unlikely since 3 mM and 0.2 mM ATP caused the same decrease in fluorescence.

The experiment was repeated with TNP-ADP (Figure 4). The fluorescence enhancement for TNP-ADP was much less than for TNP-adenosine. This was either due to a difference in TNP-adenosine and TNP-ADP affinity or to a difference in the fluorescence of protein-bound TNP-adenosine and TNP-ADP. The fluorescence change when TNP-ADP was added showed a lag phase which was removed by addition of ATP. This result is consistent with the interpretation that TNP-ADP bound tightly to the ATPase active site exhibiting no TNP fluorescence but that a lower affinity site did give rise to the fluorescence.

If TNP-adenosine or excess TNP-ADP was mixed with subfragment 1, the visible spectrum due to the Meisenheimer complex slowly disappeared, and a new absorption peak at 330 nm appeared. The initial reaction rate was measured from the rate of disappearance of the Meisenheimer complex and was 2×10^{-9} M s^{-1} for 50 μM subfragment 1 and 67 μM TNP-adenosine at pH 8 and 23 °C which corresponds to a second-order rate constant of 0.6 M^{-1} s^{-1}. The rate increased 2-fold on lowering the pH from 8 to 6.5 and about 2-fold on adding MgATP to subfragment 1.

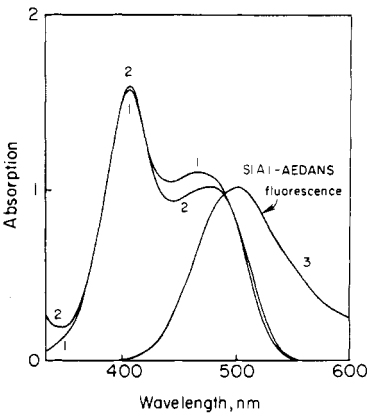

FIGURE 5: Absorption spectra of (1) 60 μM TNP-ADP and (2) 60 μM TNP-ADP and 93 μM subfragment 1 and (3) corrected emission spectrum of 1 μM S1A1-AEDANS on excitation at 340 nm. The solvent was 0.1 M KCl, 5 mM $MgCl_2$, and 50 mM Tris-HCl at pH 7.8 and 15 °C.

This phenomenon suggested that a reaction had occurred between an amino acid side chain of the protein and the TNP moiety. A number of amino acids with potentially reactive side chains were tested, but only cysteine gives any appreciable reaction. The reaction was followed by the disappearance of the visible absorption due to the Meisenheimer complex and also by the appearance of an absorption band at 330 nm (ϵ = 1.5 mM^{-1} cm^{-1}). TNP-adenosine reacted with cysteine at pH 8 and 23 °C with a second-order rate constant of 0.27 M^{-1} s^{-1}. The reaction had the same pH rate dependence as the reaction of TNP-adenosine with subfragment 1.

The most likely thiol group on subfragment 1 to have reacted covalently with TNP-adenosine is SH_1. Two experiments were carried out to test this. First, the K^+-ATPase and Ca^{2+}-ATPase activities were measured after incubating 80 μM subfragment 1 with 85 μM TNP-adenosine for 24 h in the presence of 1 mM ADP, 0.1 M KCl, 5 mM $MgCl_2$, and 20 mM 2-(*N*-morpholino)ethanesulfonic acid at pH 6.5 and 0 °C. After this time the visible absorption spectrum of TNP-adenosine had decreased by 50%. The K^+-ATPase activity had dropped to 57% and the Ca^{2+}-ATPase activity risen to 178% of control values. These activities indicate that the SH_1 group had been modified (cf. *N*-Ethylmaleimide Labeling of Subfragment 1 under Materials and Methods). Second, labeling of SH_1 by *N*-ethylmaleimide reduced the rate of the reaction of TNP-adenosine with subfragment 1 by 30%, indicating that SH_1 is one site of the reaction. In the presence of 1 mM ADP the effect was more marked, a 63% reduction in the rate being observed. However, the results also suggested that the reaction of the protein with TNP-adenosine was rather nonspecific, and other thiol groups were presumably labeled.

To determine the effect of blocking SH_1 on the weak binding site, the intensity of TNP fluorescence was measured when 44.5 μM TNP-adenosine was added to 20 μM subfragment 1 with and without *N*-ethylmaleimide labeling. The fluorescence intensity was identical in the two cases, suggesting the weak binding site is separate from the reactive site for TNP-adenosine.

Spectral Properties of the Probes. On the basis of the above chemical and thermodynamic binding data of the two probes, it was now possible to establish conditions appropriate for energy-transfer measurements. The S1A1-AEDANS corrected fluorescence emission spectrum is shown in Figure 5 as are the absorption spectra of TNP-ADP bound to the active site of subfragment 1 and also free in solution. When TNP-ADP was bound at the active site, the extinction coefficient

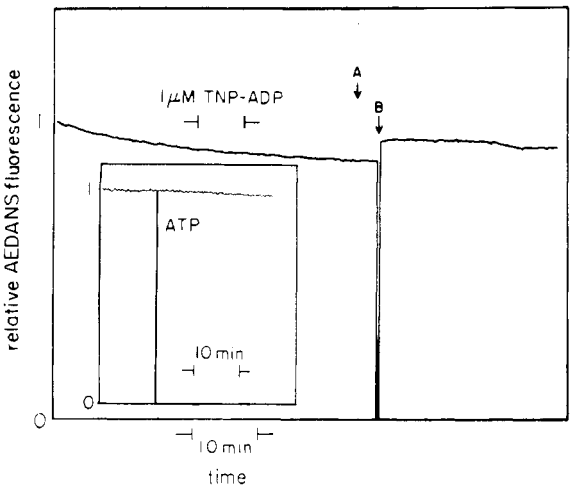

FIGURE 6: Titration of TNP-ADP into S1A1 AEDANS. Titration of TNP-ADP at a rate of 0.14 μM/min into 2 mL of 1 μM S1A1-AEDANS in 0.1 M KCl, 5 mM $MgCl_2$, and 50 mM Tris-HCl at pH 7.5 and 15 °C. (A) marks the end of the titration and (B) the addition of 4 μL of 17.8 mM ATP to give 35 μM ATP. Excitation and emission wavelengths were 340 and 560 nm, respectively. The final absorbance was 0.018 (340 nm) and <0.001 (560 nm). Inset shows the addition of 4 μL of 17.8 mM ATP to 1 μM S1A1-AEDANS under the same conditions.

of its long wavelength peak was decreased from 18.5 to 17.2 mM^{-1} cm^{-1}, and its λ_{max} was shifted from 470 to 477 nm. From the spectra the overlap integral, $J(v)$, over the range 400–700 nm was calculated to be $J(v) = 5.9 \times 10^{-14}$ cm^3 M^{-1}. The quantum yield of S1A1-AEDANS excited at 340 nm was 0.34 based on comparison with quinine bisulfate.

Efficiency of Energy Transfer. The efficiency of energy transfer between AEDANS on the light chain and TNP-ADP at the active site was calculated in two ways. The quantum yield of AEDANS was determined from steady-state and lifetime fluorescence measurements, each assay being in the presence and absence of TNP-ADP. The efficiency of energy transfer, E, was then determined from

$$E = \frac{\phi_D - \phi_{DA}}{\phi_D}$$

or

$$E = \frac{\tau_D - \tau_{DA}}{\tau_D}$$

where ϕ_D is the quantum yield of AEDANS alone and ϕ_{DA} that in the presence of acceptor and τ_D and τ_{DA} are the corresponding lifetimes. When TNP-ADP was titrated into 1 μM S1A1-AEDANS, a decrease in AEDANS fluorescence was observed (Figure 6). The wavelengths used to monitor the change in intensity were 340 nm for excitation and 560 nm for emission to avoid the TNP-ADP absorption bands. ATP was added at the end of the titration to displace the TNP-ADP from the active site. The increment in fluorescence on ATP addition was taken as the change due to energy transfer when TNP-ADP bound to S1A1-AEDANS. The inset to Figure 6 shows that ATP itself caused no change in the S1A1-AEDANS fluorescence at 560 nm. The fluorescence on ATP addition (point B, Figure 6) did not return to the starting value, the additional quenching being probably due to trivial absorption by TNP-ADP free in solution. TNP-ADP fluorescence did not contribute to the observed fluorescence. Titrations on two different S1A1-AEDANS preparations gave an efficiency of energy transfer of 0.09 and 0.085. The experiment shown in the inset of Figure 6 was repeated with five further preparations. No change in the fluorescence of S1A1-AEDANS was observed when ADP was added instead of ATP.

Table I: S1A1-AEDANS Lifetime with Various Nucleotide Ligands[a]

ligand	lifetime (ns)	SD	n
none	13.96	0.25	11
ADP	13.78	0.07	4
ATP	13.12	0.08	6
TNP-ADP	12.63	0.28	5

[a] These measurements were performed over a range of subfragment 1 (1–10 μM), ADP (14–400 μM), and ATP (100–1000 μM) concentrations. The TNP-ADP concentration was 13.3 μM. The aqueous solution contained 0.1 M KCl, 5 mM $MgCl_2$, and 50 mM Tris-HCl at pH 7.6 and 15 °C. In some cases the AEDANS lifetime was measured in the presence of 13.3 μM TNP-ADP and a large excess of ATP or ADP. In these cases ATP or ADP was assumed to be the ligand.

In order to relate the change in fluorescence intensity of S1A1-AEDANS due to TNP-ADP binding at the active site to a change in quantum yield, the shape of the overall emission spectrum must be measured with and without TNP-ADP bound. To do this and at the same time avoid the complications introduced by the relatively high absorption of TNP-ADP in the 480-nm region, the following experiment was done. The emission spectrum of 10 μM S1A1-AEDANS and 10 μM TNP-ADP in the same solvent as that used in Figure 6 was compared with the spectrum of the same solution plus 1 mM ATP (which displaced TNP-ADP from the active site). No change in the shape of the emission spectrum was observed. Hence, the fluorescence change at 560 nm can be assigned to a change in quantum yield since the intensity measured at 560 nm is directly proportional to the total fluorescence over all wavelengths (which is the actual indicator of quantum yield).

The efficiency calculated from these experiments is a minimum value since the results were uncorrected for any S1A1-AEDANS that had no bound acceptor. From the K_D one would predict that 90–95% of the subfragment 1 would have bound nucleotide. However, it is also possible that there was a small percentage of partially denatured protein. The maximum error is probably less than 20%, and as seen below, the lifetime measurements gave similar results.

The fluorescence lifetime of AEDANS covalently attached to subfragment 1 was in the region of 14 ns. The fluorescence lifetime of AEDANS can under some conditions be resolved into two components, one of about 4 ns and one much slower (Hudson & Weber, 1973). In the case of AEDANS covalently attached to subfragment 1 the amplitude of the faster component was small, and therefore, the two lifetimes could only occasionally be resolved. Normally an analysis based on a single lifetime plus a scattering component gave the best fit to the data. A typical experiment consisted of measuring the lifetime of 10 μM S1A1-AEDANS and then repeating the measurement after the addition of TNP-ADP to a concentration of 14 μM. Lifetime measurements were then made following displacement of TNP-ADP by either a large excess of ATP (1 mM) or ADP (0.4 mM).

A consistent decrease in the decay time of AEDANS was observed in the presence of TNP-ADP. The addition of ATP to the system only partially reversed this decrease, but the addition of ATP itself to S1A1 alone generally caused a slight decrease in the lifetime, so full reversal is not therefore anticipated. Further experiments were performed with 14 μM ADP in place of TNP-ADP and with addition of 400 μM ADP to displace the TNP-ADP. The average results of a large number of experiments are shown in Table I, and an example

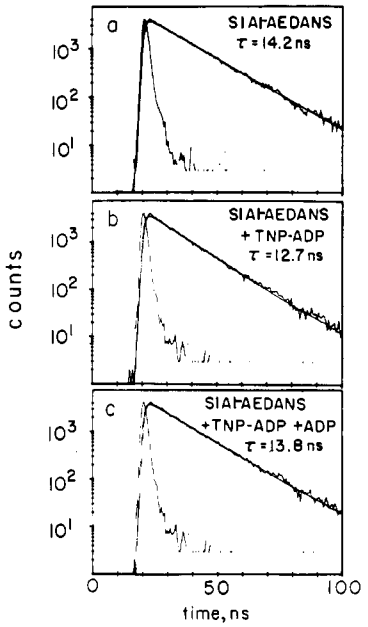

FIGURE 7: Energy transfer by fluorescence lifetime measurements. The fluorescence lifetime of the AEDANS group was measured as described under Materials and Methods in the following solutions: (a) 10.5 μM S1A1-AEDANS, (b) 10.5 μM S1A1-AEDANS and 13.3 μM TNP-ADP, (c) 10.5 μM S1A1-AEDANS, 13.3 μM TNP-ADP, and 0.4 mM ADP, each in 0.1 M KCl, 5 mM $MgCl_2$, and 50 mM Tris-HCl at pH 7.5 and 15 °C. Each panel of the figure shows the lamp flash function, the raw data, and the calculated curve with the lifetime indicated.

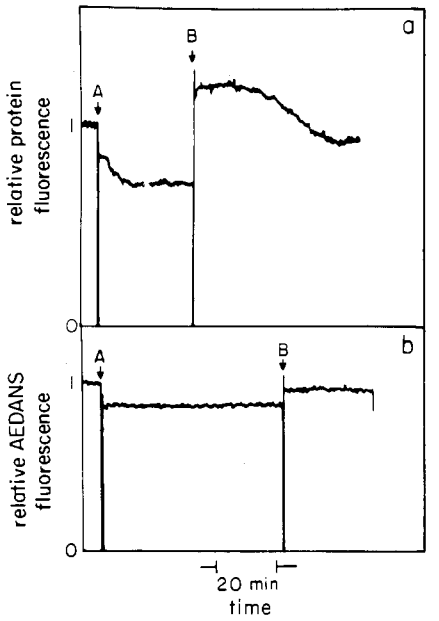

FIGURE 8: Protein and AEDANS fluorescence on addition of a 10-fold molar excess of TNP-ATP to S1A1-AEDANS. (A) marks the addition of 1.7 μL of 8.85 mM TNP-ATP to 1.5 mL of 1 μM S1A1-AEDANS in 0.1 M KCl, 5 mM $MgCl_2$, and 50 mM Tris-HCl at pH 7.5 and 15 °C. (B) marks the addition of 1.5 μL of 17.8 mM ATP to give 18 μM ATP. Upper trace shows protein fluorescence with excitation and emission wavelength of 300 and 340 nm, respectively. Lower trace shows AEDANS fluorescence with excitation and emission weavelengths of 340 and 560 nm, respectively.

of a specific experiment is shown in Figure 7. ADP had little or no effect on the AEDANS lifetime while TNP-ADP decreased the lifetime by approximately 10%. As already noted ATP also decreased the lifetime by approximately 6%. We observed no effect of 1 mM ATP on the AEDANS fluorescence in a steady-state measurement (see insert of Figure 6). This lack of correlation between the steady-state and lifetime measurements when ATP is added to S1A1-AEDANS remains to be explained.

The efficiency of energy transfer was determined from lifetime measurements on the same two preparations of S1A1-AEDANS used in the titration experiments. The efficiences of transfer were 0.10 and 0.08 so that in each preparation there was good agreement between the results from the steady-state quantum yield experiment and the life-time experiment. The efficiency of energy transfer was taken from these data to be 0.09.

Energy Transfer in Two Different Subfragment 1 Nucleotide Complexes. A principal aim of this work was to investigate how the efficiency of energy transfer varied in different myosin nucleotide complexes and, if possible, to correlate any changes seen with changes in the distance between the chromophores.

The quantum yield of AEDANS fluorescence was compared during steady-state S1A1-AEDANS-catalyzed hydrolysis of TNP-ATP and when TNP-ADP was bound to the protein. When 10-fold molar excess of TNP-ATP was added to S1A1-AEDANS, an initial rapid drop in protein fluorescence was observed followed by a steady phase and a second but slow decrease in fluorescence after 3 min (Figure 8a). Our interpretation is that TNP-ATP rapidly bound to S1A1-AEDANS to give a steady-state complex and then slowly decayed to the TNP-ADP bound state. On the other hand, when the experiment was repeated, AEDANS emission (Figure 8b) showed no detectable change in intensity, and so the efficiencies of energy transfer for both the steady-state complex and for protein-bound TNP-ADP were the same.

To check the above interpretation regarding which states were being observed, the dissociation rate constant of TNP-ADP from subfragment 1 was measured in a stopped-flow experiment and compared with the steady-state TNP-ATPase rate; 10 μM TNP-ADP was displaced from 10 μM subfragment 1 by either 100 μM or 5 mM ATP in the same solvent as used in the above experiment (Figure 8). In each case the observed exponential process had a rate constant of 7 s^{-1}. This is more than an order of magnitude greater than the catalytic center activity of the TNP-ATPase under these conditions (cf. 0.4 s^{-1} in Figure 8a from the time of addition of TNP-ATP to when the steady-state phase is over).

In agreement with the conclusion of Hiratsuka & Uchida (1973), it appears that the steady-state complex during TNP-ATP-catalyzed hydrolysis is not simply a protein–TNP-ADP complex. It is most likely a mixture of protein–TNP-ATP and protein–products complexes by analogy with the situation when ATP is substrate.

Lifetime Measurements with TNP-adenosine. Early titration results had suggested that the weak binding site of TNP-ADP was close enough to Cys-177 for energy transfer to occur. However, the results were difficult to interpret because very large correction factors for absorption are required. An indication that the weak binding site is close to the AEDANS on the alkali light chain was obtained from fluorescent lifetime measurements.

As noted above, the fluorescence decay of S1A1-AEDANS is characterized by a single lifetime. When a large excess of TNP-adenosine was added, two lifetimes were observed. Our interpretation is that the faster one is derived from S1A1-AEDANS with TNP-adenosine bound and the slower one from free S1A1-AEDANS (Table II). The lifetimes indicated that TNP-adenosine bound at the weak site quenched AEDANS fluorescence by 50–80%. It was not possible to be more precise in estimating the degree of energy transfer, since the

Table II: S1A1-AEDANS Lifetimes in the Presence of TNP-adenosine[a]

nucleoside additions	τ_1 (ns)	A_1	τ_2 (ns)	A_2
none			14.1	1
60 μM TNP-adenosine	6.4	0.39	14.4	0.61
60 μM TNP-adenosine + 1 mM ATP	9.5	0.58	15.5	0.42

[a] Fluorescence lifetimes (τ_1, τ_2) were measured as described under Materials and Methods. A_1 and A_2 are normalized preexponential factors. The solutions contained TNP-adenosine and ATP as shown, 20 μM S1A1-AEDANS, 0.1 M KCl, 5 mM $MgCl_2$, and 50 mM Tris-HCl at pH 7.6 and 15 °C.

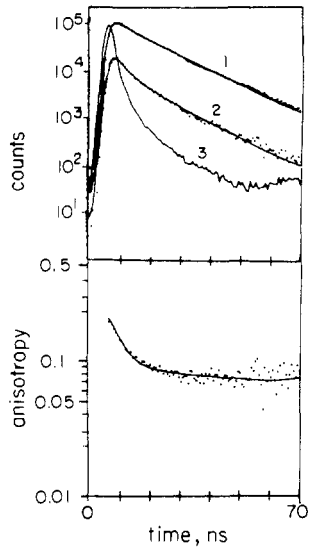

FIGURE 9: Measurement of the time-dependent anisotropy of 11 μM S1A1-AEDANS at 8 °C in 0.1 M KCl, 5 mM $MgCl_2$, and 50 mM Tris-HCl at pH 7.6. The upper frame shows the intensity of emission: (1) $I_\parallel + 2I_\perp$; (2) $I_\parallel - I_\perp$. Trace 3 shows the lamp flash function. The lower frame shows the anisotropy computed from (1) and (2). The points represent the data, and the lines are the best fit to the data.

fraction of S1A1-AEDANS containing bound TNP-adenosine was also unknown, and hence, the relative amplitudes and the lifetimes of the two phases of the fluorescence decay both had to be evaluated from the records.

Time-Dependent Fluorescence Anisotropy Measurement of S1A1-AEDANS. The time-dependent anisotropy of S1A1-AEDANS was measured at 8 °C over 8 h. The results shown in Figure 9 demonstrate the biphasic nature of the decay in anisotropy. The slow rotational correlation function of about 180 ns (note that the data points in Figure 9 are scattered after 40 ns) corresponds to the motion of the whole protein (Mendelson et al., 1973). The fast decay time of 4 ns is interpreted as being due to the motion of the AEDANS with respect to the protein or of local segmental motion of the protein. The zero motion anisotropy, A_f, was computed from the data to be 0.32.

The relative amplitudes of the two rotational correlation functions are such that a large part of the decay in the anisotropy is due to the rapid decay function. Thus, the AEDANS has considerable freedom of motion relative to subfragment 1.

Discussion

Energy-transfer measurements require the specific incorporation of the donor and acceptor molecules; therefore, the specificity of the labeling of the alkali light chains was examined in some detail. Examination of the elution profile of the peptides resulting from tryptic digestion of the light chains strongly suggests that the labeling occurs at a unique site presumably at Cys-177 (Figure 1).

The interactions of the acceptor TNP-ADP with subfragment 1 are more complex. The data indicate that there are three sites in subfragment 1 which can interact with TNP-ADP: the active site, a weak binding site, and the SH_1 thiol residue.

The interaction of TNP-ADP with heavy meromyosin has been studied previously (Hiratsuka, 1976). The K_D was found to be 0.8 μM based on a titration curve by using TNP fluorescence enhancement, but no evidence was presented for a weak binding site. The possible effect of absorption on the observed fluorescence was not discussed, even though the excitation wavelength was 460 nm. It seems likely that the second binding site was not seen due to the high absorbance of the solution. Our data suggest that TNP fluorescence is associated predominately with binding at the weak site rather that at the active site.

TNP fluorescence can be used as a sensitive indication of binding at the second site. With dilute protein and TNP-nucleotide solutions the active site can be saturated essentially without occupancy at the weak site. Thus, it was possible to determine conditions for energy-transfer measurements involving TNP absorption solely at the active site.

The reaction of TNP-ADP at the SH_1 thiol is slow at pH 7.6 on the time scale of the energy-transfer experiments. The concentration of TNP-ADP would not have changed significantly during the course of any experiments in which energy transfer was measured. In any event any TNP-ADP which might have reacted would have lost its visible absorption band and be nonfluorescent and so would not interfere with the energy-transfer measurements. The weak binding site does not seem to be related to reaction at the SH_1 thiol, and there is little indication of its location on the subfragment 1 molecule. The energy-transfer measurements with TNP-adenosine indicate that this site is quite close (<40 Å) to AEDANS and, hence, to Cys-177. Tao & Lamkin (1981) also suggested there is a TNP-nucleotide weak binding site from their Förster energy-transfer studies. They found that the fluorescence of AEDANS attached to the SH_1 thiol was quenched by TNP-AMP even when ADP or ATP was bound at the ATPase active site.

The efficiency of energy transfer between probes at the ATPase active site and the alkali light chain thiol was determined by both quantum yield and fluorescence lifetime measurements. The agreement between the two methods indicates that the energy transfer measured is a function of the distance between the light chain thiol and the active site and not, for example, due to a small percentage of the nucleotide bound at the weak site.

R_0, the distance at which the efficiency of energy transfer is 50%, was calculated from

$$R_0^6 = \frac{(8.78 \times 10^{-25})K^2\phi_D J(\upsilon)}{n^4}$$

where n = refractive index.

The quantum yield of S1A1-AEDANS, ϕ_D, was measured to be 0.34; however, comparison of the S1A1-AEDANS lifetime with the data of Hudson & Weber (1973) suggested that the quantum yield could be as high as 0.46. A value of 0.4 was used. The refractive index for a protein was taken to be 1.4.

The absence of change in the efficiency of energy transfer between the active site and the AEDANS in different nucleotide complexes suggests that any structural changes be-

tween the complexes do not extend as far as Cys-177. The possibility that a change in distance is compensated for by a change in K^2 is unlikely but cannot be ruled out.

The amplitude of the decay of anisotropy due to protein motion can be used to restrict the possible range of value for K^2 by using the method developed by Dale & Eisinger (1975). Thus, a depolarization factor, D, can be calculated from $D = A_0/A_f$ where $A_0 \approx 0.1$ (the zero time anisotropy extrapolated from the slower phase of Figure 9) and $A_f = 0.32$ (the zero motion anisotropy). This value for A_f is less than the theoretical value of 0.4 probably because the polarization across the excitation spectrum of AEDANS shows two overlapping electronic transitions (Hudson & Weber, 1973). The value of 0.32 is the same as that estimated by Wu et al. (1976). The broad excitation band used in the experiment to measure the anisotropy of S1A1-AEDANS would excite both electronic transitions, thus lowering the zero motion anisotropy.

When a model is assumed whereby the AEDANS moves through the volume of a cone (Kawato et al., 1977), the half-angle of the cone is calculated to be 48°. This leads to a range for K^2 of between 0.28 and 1.65 assuming the second dipole is fixed. The chemical structure of TNP-ADP suggests that the chromophore will be quite rigid with respect to the protein, since there is no bond between the chromophore and the ribose ring about which free rotation can occur. Nevertheless, the current understanding of local motion in proteins suggests it is unlikely there will be zero mobility (McCammon et al., 1979). In addition TNP-ADP has two dipoles because it has two absorption peaks, and both dipoles can act as the energy acceptor. Each of these factors probably contributes to alleviating the problem of assigning a value to K^2.

Thus, it is likely that K^2 will approximately equal $^2/_3$. This has generally been an appropriate value of K^2 for distance measurements in proteins (Stryer, 1978) even when uncertainty exists as to the freedom of motion of the probes. We will therefore perform calculations based on $K^2 = {}^2/_3$ and compare the results with those obtained using limits of $0.28 < K^2 < 1.65$. For $K^2 = {}^2/_3$, $R_0 = 39$ Å. For $0.28 < K^2 < 1.65$, 34 Å $< R_0 <$ 46 Å.

The range is further widened if the value of ϕ_D is extended to cover the range of the two estimates from 0.34 to 0.46, in which case 33 Å $< R_0 <$ 47 Å. E (=0.09) is related to the distance between the dipoles by

$$E = 1/[1 + (R/R_0)^6]$$

from which it follows that $R = 57$ Å, with limits 48 Å $< R <$ 69 Å.

In defining the distance between probes on subfragment 1, it is appropriate to consider the variation in the location of the probes with respect to the protein. As noted above, the position of TNP-ADP is probably relatively invariant. The AEDANS group, however, is joined to the protein by a 10-Å flexible chain giving rise to considerable potential mobility of the AEDANS. For the model in which AEDANS moves through a cone of half-angle of 48°, an AEDANS dipole could change its position by about 15 Å across the surface of the protein and vary its distance from the protein by about 5 Å due to the flexible chain. If segmental motion of the protein also occurs, this range would be even greater.

It has been shown (Steinberg & Katchalski-Katzir, 1968; Elkana et al., 1968) that motion of this type between the donor and acceptor molecules will enhance the energy transfer seen. Thomas et al. (1978) give 10^{-6}–10^{-5} cm^2 s^{-1} (=10–100 Å^2 ns^{-1}) as the diffusion coefficient for small molecules in an aqueous solution. Therefore, a probe with a lifetime of 14 ns could diffuse many times through the volume of a cone 15 Å in diameter, and so the efficiency of energy transfer would be enhanced [i.e., the distance may correspond to that of closest approach between the probes rather than the average separation (Haas et al., 1978)]. However, the rate of diffusion of the probe close to the surface of a protein may be less than the rate in free solution.

The above discussion highlights the uncertainties inherent in the distance measurement reported here. Nevertheless, when all the data are taken together, a useful picture emerges of intramolecular distances within subfragment 1 (Morales et al., 1982). The characterization of the ATP binding site by Okamoto & Yount (1983) is a further significant step in relating the alkali-light chain–ATPase active site distance to the subfragment 1 structure.

The failure to detect distance changes across subfragment 1 during ATPase activity is not unexpected from current knowledge of the structural changes occurring during ATPase activity. Nevertheless, Marsh et al. (1982) have shown that certain interactions of subfragment 1 can be transmitted within a cycle of ATPase activity from the ATPase active site to probes attached to the alkali light chain at Cys-177. Dalbey (1983) has shown that the distance between the thiols, SH_1 and SH_2, on the heavy chain probably decreases by several angstroms when nucleotides bind at the ATPase active site. From the perspective of cross-bridge motion, it seems likely that, if significant inter- and intramolecular motions occur and are to be detected by these techniques during ATPase activity, then the preparation of cross-linked actin and subfragment 1 described by Mornet et al. (1981) will be most useful.

Acknowledgments

We thank Dr. J. M. Vanderkooi for help with the time-resolved fluorescence and the anisotropy measurements.

Registry No. 1,5-IAEDANS, 36930-63-9; TNP-ADP, 77450-67-0; TNP-ATP, 61368-63-6; TNP-adenosine, 77450-69-2; Cys, 52-90-4; ATPase, 9000-83-3.

References

Azegami, M., & Iwai, K. (1964) *J. Biochem. (Tokyo) 55*, 346–348.

Burke, M., & Reisler, E. (1977) *Biochemistry 16*, 5559–5563.

Dalbey, R. (1983) *Biophys. J. 41*, 98a.

Dale, R. E., & Eisinger, J. (1975) *Biochem. Fluoresc.: Concepts 1*, 116–284.

Dixit, B. P. S. N., Waring, A. J., Wells, K. O., Wong, P. S., Woodrow, G. V., & Vanderkooi, J. M. (1982) *Eur. J. Biochem. 126*, 1–9.

Elkana, Y., Feitelson, J., & Katchalski, E. (1968) *J. Chem. Phys. 48*, 2399–2404.

Frank, G., & Weeds, A. G. (1974) *Eur. J. Biochem. 44*, 317–334.

Gafni, A., Modlin, R. L., & Brand, L. (1975) *Biophys. J. 15*, 263–280.

Gratzer, W. G., & Lowey, S. (1969) *J. Biol. Chem. 244*, 22–25.

Haas, E., Katchalski-Katzir, E., & Steinberg, I. Z. (1978) *Biopolymers 17*, 11–31.

Hiratsuka, T. (1976) *Biochim. Biophys. Acta 453*, 293–297.

Hiratsuka, T., & Uchida, K. (1973) *Biochim. Biophys. Acta 320*, 635–647.

Hudson, E., & Weber, G. (1973) *Biochemistry 12*, 4154–4161.

Kawato, S., Kinosita, K., & Igegami, A. (1977) *Biochemistry 16*, 2319–2324.

Marsh, D. J., & Lowey, S. (1980) *Biochemistry 19*, 774–784.

Marsh, D. J., Stein, L. A., Eisenberg, E., & Lowey, S. (1982) *Biochemistry 21*, 1925–1928.

McCammon, J. A., Wolynes, P. G., & Karplus, M. (1979) *Biochemistry 18*, 927–942.
Mendelson, R. A., Morales, M. F., & Botts, J. (1973) *Biochemistry 12*, 2250–2255.
Morales, M. F., Borejdo, J., Botts, J., Cooke, R., Mendelson, R. A., & Takashi, R. (1982) *Annu. Rev. Phys. Chem. 33*, 319–351.
Mornet, D., Betrand, R., Pantel, P., Audemard, E., & Kassab, R. (1981) *Nature (London) 292*, 301–306.
Moss, D. J., & Trentham, D. R. (1980) *Fed. Proc., Fed. Am. Soc. Exp. Biol. 39*, 1935.
Okamoto, Y., & Yount, R. G. (1983) *Biophys. J. 41*, 298a.
Parker, C. A. (1968) in *Photoluminescence of Solutions*, pp 261–268, Elsevier, Amsterdam.
Perrie, W. T., Smillie, L. B., & Perry, S. V. (1973) *Biochem. J. 135*, 151–154.
Scott, T. G., Spencer, R. D., Leonard, N. J., & Weber, G. (1970) *J. Am. Chem. Soc. 92*, 687–695.
Smyth, D. G. (1967) *Methods Enzymol. 11*, 214–231.
Steinberg, I. Z., & Katchalski-Katzir, E. (1968) *J. Chem. Phys. 48*, 2404–2410.
Stryer, L. (1978) *Annu. Rev. Biochem. 47*, 819–846.
Tao, T., & Lamkin, M. (1981) *Biochemistry 21*, 5051–5055.
Taylor, E. W. (1979) *CRC Crit. Rev. Biochem. 6*, 103–164.
Thomas, D. D., Carlson, W. F., & Stryer, L. (1978) *Proc. Natl. Acad. Sci. U.S.A. 75*, 5746–5750.
Trentham, D. R., Eccleston, J. F., & Bagshaw, C. R. (1976) *Q. Rev. Biophys. 9*, 217–281.
Vanderkooi, J. M., Ierokamas, A., Nakamuro, H., & Martinosi, A. (1977) *Biochemistry 16*, 1262–1267.
Wagner, P. D., & Weeds, A. G. (1977) *J. Mol. Biol. 109*, 455–473.
Watterson, J. G., Schaub, M. C., Locher, R., Di Pierri, S., & Kutzer, M. (1975) *Eur. J. Biochem. 56*, 79–90.
Webb, M. R., & Trentham, D. R. (1983) in *The Handbook of Physiology; Skeletal Muscle* (Peachey, L. D., Adrian, H., & Geiger, S. R., Eds.) pp 237–255, American Physiological Society, Bethesda, MD.
Weeds, A. G. (1976) *Eur. J. Biochem. 66*, 157–173.
Weeds, A. G., & Taylor, R. S. (1975) *Nature (London) 257*, 54–56.
Weeds, A. G., & Pope, B. (1977) *J. Mol. Biol. 111*, 129–157.
Wells, J. A., & Yount, R. G. (1979) *Proc. Natl. Acad. Sci. U.S.A. 76*, 4966–4970.
Whitaker, J. R., Yates, D. W., Bennett, N. G., Holbrook, J. J., & Gutfreund, H. (1974) *Biochem. J. 139*, 677–697.
Wu, C. W., Yarbrough, L. R., Wu, F. Y.-H., & Hillel, Z. (1976) *Biochemistry 15*, 2097–2104.

Laser Flash Photolysis Studies of Intramolecular Electron Transfer in Milk Xanthine Oxidase†

Anjan Bhattacharyya, Gordon Tollin,* Michael Davis, and Dale E. Edmondson

ABSTRACT: The laser flash photolysis technique has been used to study the reaction of the 5-deazaflavin radical with the redox centers of milk xanthine oxidase under anaerobic conditions. Kinetic studies show that the deazaflavin radical reacts primarily with the functional Mo center, the FAD moiety, and, to a small extent, the Fe/S_I center. The reaction of the photogenerated reductant with the functional Mo center is second order ($k = 6.6 \times 10^7$ M^{-1} s^{-1}), whereas its reaction with the FAD moiety is more rapid ($t_{1/2} < 25$ μs), apparently occurring via a preexisting complex. No evidence was found for the Mo reaction of the 5-deazaflavin radical with the desulfo-Mo center or when the Mo was trapped as Mo^{IV} by complexation with alloxanthine. Kinetic traces observed at 483 nm show the reduction of the two Fe/S centers to be bisphasic, with Fe/S_I being reduced more rapidly ($k = 77$ s^{-1}) than Fe/S_{II} ($k = 12$ s^{-1}). No evidence was found for any direct electron transfer between the two Fe/S centers. Flash photolysis studies with deflavo-xanthine oxidase show that in contrast to other forms of the enzyme which contain FAD, Fe/S_{II} can react directly with the 5-deazaflavin radical in a second-order manner. When a functional Mo center is present, Fe/S reduction occurs either via direct reaction with the 5-deazaflavin radical or via reaction with Mo^V. In the desulfo-deflavoenzyme, reduction of the two Fe/S centers occurs only by direct reaction with the 5-deazaflavin radical. From an analysis of the kinetic data and the reported oxidation–reduction potentials of the centers in xanthine oxidase, the forward and reverse rate constants for each of the inter- and intramolecular electron-transfer processes have been calculated. The results obtained on the one-electron reduced form of the enzyme are inconsistent with the views that (1) equilibration of reducing equivalents among the redox centers in xanthine oxidase occurs much more rapidly than turnover and (2) the distribution observed among the various centers during rapid mixing experiments is dependent on their relative oxidation–reduction potentials.

Mechanistic studies of inter- and intramolecular electron-transfer reactions in enzymes containing multiple redox centers have been and continue to be an area of active research interest (Palmer & Olson, 1980). Due to its ready availability and stability, milk xanthine oxidase has been the subject of numerous kinetic and structural studies [cf. Bray (1975, 1980)]. The enzyme contains one molybdenum, one FAD, and two 2Fe–2S centers in each of its two independent catalytic centers. The Mo center is now generally accepted to be the site of entry of reducing equivalents from the substrate, while the FAD moiety is the site of reduction of O_2 via either a two-electron or a one-electron mechanism (Hille & Massey, 1981; Porras et al., 1981). Results from studies on the deflavo

† From the Department of Biochemistry, University of Arizona, Tucson, Arizona 85721 (A.B. and G.T.), and the Department of Biochemistry, Emory University, School of Medicine, Atlanta, Georgia 30322 (M.D. and D.E.E.). *Received March 30, 1983.* This research was supported in part by grants from the National Institutes of Health (AM15057 to G.T. and GM29433 to D.E.E.) and the National Science Foundation (PCM81007700 to D.E.E.).

0006-2960/83/0422-5270$01.50/0